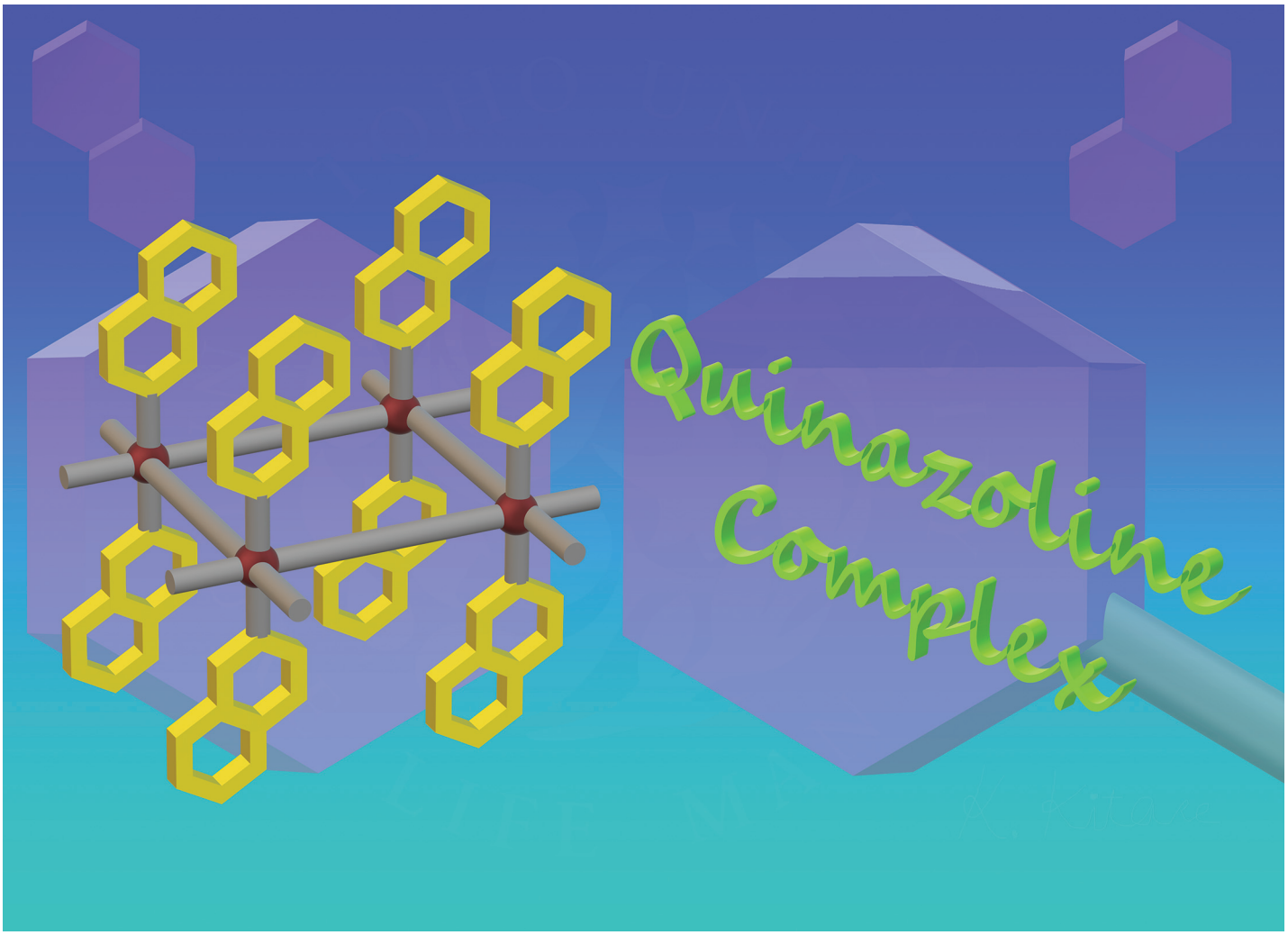

Showcasing research from Professor Kitazawa's laboratory, Department of Chemistry, Toho University, Chiba, Japan.

Soma–Iwamoto-type SCO complex $Fe(quinazoline)_2[Au(CN)_2]_2$ using the quinazoline-type ligand

In our current work, we have synthesized a novel Soma–Iwamoto-type complex, $Fe(quinazoline)_2[Au(CN)_2]_2$. This complex shows the Soma–Iwamoto-type bilayer with Au–Au interactions and a gradual spin-crossover (SCO) phenomenon. A small amount of crystals of $Fe(H_2O)_2(quinazoline)_2[Au(CN)_2]_2$ has also been obtained, using the filter method, and found to have a mononuclear structure with a hydrogen-bonding network. The difference between these structures can be explained by the difference between the concentrations of the quinazoline ligand during their syntheses.

As featured in:

See Kosuke Kitase *et al.*, *Dalton Trans.*, 2024, **53**, 9248.

ROYAL SOCIETY OF CHEMISTRY

rsc.li/dalton

Registered charity number: 207890

Dalton Transactions

ROYAL SOCIETY OF CHEMISTRY

COMMUNICATION

View Article Online
View Journal | View Issue

Check for updates

Cite this: *Dalton Trans.*, 2024, **53**, 9248

Received 16th February 2024,
Accepted 18th April 2024

DOI: 10.1039/d4dt00458b

rsc.li/dalton

Soma–Iwamoto-type SCO complex $Fe(quinazoline)_2[Au(CN)_2]_2$ using the quinazoline-type ligand†

Kosuke Kitase, *[a] Daisuke Akahoshi[b] and Takafumi Kitazawa[a,c]

The Hofmann-type complex and Soma–Iwamoto-type complex are cyano-bridged coordination polymers and both have been widely researched. Now we have synthesized a novel Soma–Iwamoto-type complex, namely $Fe(quinazoline)_2[Au(CN)_2]_2$. This complex shows the Soma–Iwamoto-type bilayer with Au–Au interactions and a SCO phenomenon with a gradual change of magnetic susceptibility. $Fe(H_2O)_2(quinazoline)_2[Au(CN)_2]_2$ has also been synthesized and crystallized, and has been found to be a mononuclear complex with hydrogen-bonding network interactions.

Introduction

The spin-crossover (SCO) phenomenon involves a reversible spin transition between high-spin (HS) and low-spin (LS) states. The Hofmann-type complex is a coordination polymer comprising central metal ions, such as Fe, Ni, or Cd, bridging ligands $[M(CN)_4]$ (M′ = Ni, Pd, Pt), and aromatic ligands, such as pyridine or pyrazine. The first Hofmann-type complex produced was $Ni(NH_3)_2[Ni(CN)_4]\cdot 2(C_6H_6)$, reported by K. A. Hofmann.[1] The first Hofmann-type SCO complex was $Fe(Py)_2[Ni(CN)_4]$, reported by Kitazawa *et al.*[2] The Soma–Iwamoto-type complex is a derivative of the Hofmann-type complex with the square metal tetracyanide $[M(CN)_4]$ replaced by a linear metal dicyanide $[M(CN)_2]$ (M′ = Ag, Au). We suggest this type complex call "Soma–Iwamoto-type complex" because the first reported one is $[Cd(4,4'\text{-bpy})_2\{Ag(CN)_2\}_2]$[4] and the second one is $[Cd(py)_2\{Ag(CN)_2\}_2]$.[5,6] Soma and Iwamoto reported both complexes. Many laboratories have researched the Hofmann-type and Soma–Iwamoto-type complexes[2–15] due to their potential to be used as functional materials such as sensors or switching materials and due to their tunable properties.

Most reported Hofmann-type or Soma–Iwamoto-type complexes contain pyridine, pyrazine,[3] or bipyridine-type[7] ligands with all N atoms coordinated to metal atoms. However, the Hofmann-type or Soma–Iwamoto-type complexes containing other N-hetero aromatic ligands, such as imidazole[11] or pyrimidine,[12–15] have been reported much less than have complexes using pyridine, pyrazine, or bipyridine-type ligands. We previously reported Soma–Iwamoto-type SCO complexes using 4-methylpyrimidine[13,14] and 4-methoxypyrimidine.[15]

Quinazoline is a pyrimidine-type ligand, and its relatively large π-electron system could form relatively strong π–π interactions. Here, we synthesized a Soma–Iwamoto-type SCO complex, namely $Fe(quinazoline)_2[Au(CN)_2]_2$ (**1**‡) and notable with its quinazoline ligand, and determined structural and magnetic properties of this complex.

Experimental

Complex **1** was synthesized using Mohr's salt $Fe(NH_4)_2(SO_4)_2\cdot 6H_2O$, L-ascorbic acid, $K[Au(CN)_2]$, and quinazoline. A yellow powder resulted from mixing Mohr's salt with L-ascorbic acid and quinazoline in a solution. Single yellow crystals of complex **1** were grown using the slow diffusion method. Yellow single crystals were also obtained using the filter method, but in an amount so small precluding analyses other than by single-crystal X-ray diffraction. The X-ray-determined formula and structure of this complex were different from the others, so we called it "complex **2**". The details of the synthesis method used is described in ESI.†

The expected composition of the synthesized powder complex was confirmed by performing elemental analysis using J-Science MICRO CORDER JM10, complex **1**: anal. calc'd for $C_{20}H_{12}N_8FeAu_2$: C 29.50%, H 1.48%, N 13.76%. Found: C 29.27%, H 1.65%, N 13.73%. This complex was also character-

[a]*Department of Chemistry, Toho University, Chiba 274-8510, Japan. E-mail: kitazawa@chem.sci.toho-u.ac.jp*
[b]*Department of Physics, Toho University, Chiba 274-8510, Japan*
[c]*Research Centre for Materials with Integrated Properties, Toho University, Chiba 274-8510, Japan*

†Electronic supplementary information (ESI) available. CCDC 2332161–2332165. For ESI and crystallographic data in CIF or other electronic format see DOI: https://doi.org/10.1039/d4dt00458b

ized by carrying out thermogravimetric (TG) analysis using a Hitachi High-Technologies Corporation TG/DTA6200 apparatus (Fig. S1†) and powder X-ray diffraction (XRD) using a Rigaku Co. X-ray diffractometer or MAC Science M03XHF22 apparatus (Fig. S3†).

The superconducting quantum interference device method from Quantum Design MPMS-5S was used to measure the magnetic susceptibilities of these complexes at temperatures ranging from room temperature to 4 K under a 0.1 T field and a cooling rate of 1 K min^{-1}. The sample so analyzed was placed in a gelatin capsule, which was filled with a plastic straw, and the capsule was fixed by making a dent near the capsule inside the straw.

The crystal structure of complex **1** was determined by carrying out single-crystal XRD using a Bruker SMART diffractometer with a Mo-Kα line, and done so at 296 K (HS state), 150 K (intermediate state), and 90 K (LS state). The structure was solved using SHELX 2014 software.[17,18]

Results and discussion

We obtained a yellow powder sample of complex **1** and a yellow crystal of complex **1** using the slow diffusion method. However, the yellow crystal of $Fe(H_2O)_2(quinazoline)_2[Au(CN)_2]_2$ (**2**) was obtained using the filter method. That difference of formula could be explained by the difference in the concentrations of the ligands during synthesis. The production of the powder sample and single crystal using the slow diffusion method involved a high ligand concentration, but a low ligand concentration was used for the filter method. The aqueous solution of Mohr's salt and quinazoline turned yellow during synthesis of the powder sample and single crystal using the slow diffusion method. Which indicates that the Fe-quinazoline complex had formed. Therefore, we posited that complex **1** was obtained by replacing some of the quinazoline ligands of the Fe-quinazoline complex with $[Au(CN)_2]^-$ bridging ligands—but that complex **2** was obtained by substituting quinazoline ligands into a form or forms of the Fe-$[Au(CN)_2]^-$ complex, such as $\{Fe[Au(CN)_2]_3\}_n^{n-}$,[16] when producing the single crystals using the filter method. We determined the predominance of the substitution by the $[Au(CN)_2]^-$ bridging ligand in the former case to be due to the high quinazoline concentration, whereas substitution by H_2O also occurred in the latter case due to the low quinazoline concentration.

Fig. 1 displays the crystal structure of complex **1**, showing the Soma–Iwamoto-type double layer with aurophilic interactions. The space group was determined to be $P2_1/c$ at 296 K, 150 K, and 90 K. The lattice constants were determined to be as follows: a = 10.8433(10) Å, b = 14.6937(14) Å, c = 14.7279(14) Å, and β = 93.865(2)° at 296 K; a = 10.698(3) Å, b = 14.331(4) Å, c = 14.527(4) Å, and β = 94.049(4)° at 150 K; and a = 10.662(3) Å, b = 14.119(3) Å, c = 14.375(4) Å, and β = 94.257(4)° at 90 K. The Fe–N bond length was found to be shorter at lower temperatures (Table 1), indicative of the SCO phenomenon between the HS and LS states. At 150 K, the Fe–N bond length was observed to be between those at 296 K and 90 K, indicating the Fe site at 150 K to be a mixture of HS and LS states. Also, the unit cell was smaller at lower temperatures. The quinazoline ligand in complex **1** was disordered in two directions. Due to steric hindrance, all the quinazoline ligands coordinated with the metal atom using only their respective 3-position nitrogens.

Fig. 2 displays the crystal structure of complex **2**, showing a mononuclear complex with a nitrogen atom at the quinazoline 1-position, H_2O and CN–H_2O hydrogen bond network, and weak Au–Au interactions (Fig. 3 and Table 3). These interactions seems to stabilize the mononuclear structure. The Fe–

Table 1 Bond lengths of complex **1**

Average bond lengths/Å			
T/K	296(2)	150(2)	90(2)
Fe–N_{ligand}	2.213(14)	2.10(2)	2.024(18)
Fe–N_{cyano}	2.145(9)	2.034(14)	1.961(12)
Au–C	2.002(13)	2.01(2)	2.007(19)
Au–Au	3.114(8)	3.086(10)	3.040(18)

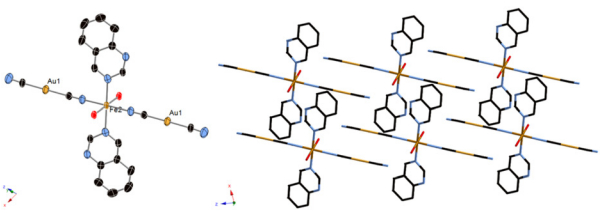

Fig. 2 Crystal structure of complex **2**. (Left: ORTEP structure. Right: packing structure along the *Y* axis.)

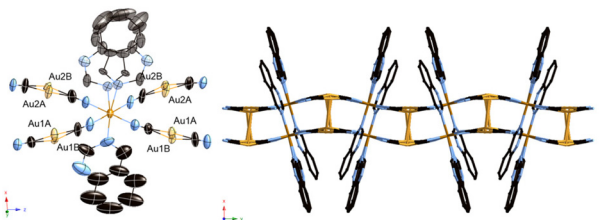

Fig. 1 Crystal structure of complex **1**. (Left: ORTEP structure. Right: packing structure along the *X* axis.)

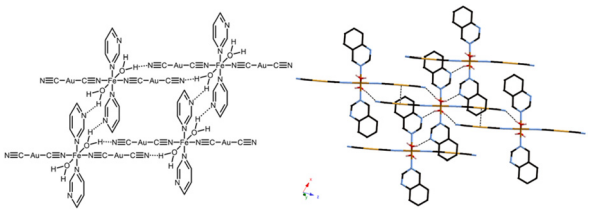

Fig. 3 Hydrogen bonding network of complex **2**.

Table 3 Hydrogen bond lengths of complex **2**

Average bond lengths/Å		
T/K	296(2)	90(2)
O–H···N_{ligand}	2.00(4)	1.99(4)
O–H···N_{cyano}	1.93(3)	1.91(3)

N bond length at 296 K and that at 90 K were observed to be similar, in the 2.1–2.3 Å range (Table 2), indicative of complex **2** not showing the SCO phenomenon, and indicative of the Fe state being HS at these two temperatures. The space group was determined to be $P\bar{1}$ at 296 K and 90 K. The lattice constants were as follows: a = 7.3203(8) Å, b = 7.8613(8) Å, c = 10.8262(12) Å, α = 81.6096(19)°, β = 77.6448(18)°, and γ = 79.8104(18)° at 296 K; a = 7.2983(11) Å, b = 7.7651(12) Å, c = 10.7931(17) Å, α = 80.236(4)°, β = 76.919(3)°, and γ = 79.867(3)° at 90 K.

Fig. 4 shows the acquired magnetic susceptibility curve of complex **1**, with the results indicating a gradual occurrence of SCO between 100 K and 200 K. The magnetic susceptibility was measured to be 3.6 cm^3 mol^{-1} K at 300 K and 0.28 cm^3 mol^{-1} K at 50 K. The magnetic susceptibility curve of complex **1** showed a two-step transition without a plateau and with the half transition point, $T_{1/2}$, at approximately 150 K. The double-layered structure might have caused this behavior. A small amount of magnetic susceptibility remained at very low temperatures—perhaps due to supramolecular interactions such as π–π interactions or due to the presence of slight amounts of non-SCO impurities as in complex **2**, with the former explanation more likely than the latter one as no peak corresponding to complex **2** was observed in the powder X-ray diffraction (Fig. S3†).

Yan-Cong Chen *et al.*[8] reported the two complexes to be isostructural, but with complex **1** displaying a transition temperature higher than that that of Fe(isoquinoline)$_2$[Au(CN)$_2$]$_2$. This behavior has been reported between Fe(4-methylpyridine)$_2$[Au(CN)$_2$]$_2$ and Fe(4-methylpyrimidine)$_2$[Au(CN)$_2$]$_2$ and can be explained by the difference in the coordination field between pyridine and pyrimidine. However, a plateau of the intermediate state was not observed in the magnetic susceptibility curve of complex **1**, despite the curve for Fe(isoquinoline)$_2$[Au(CN)$_2$]$_2$ showing a plateau at about 120 K. This result indicated the intermediate state of complex **1** to be less stable than that of Fe(isoquinoline)$_2$[Au(CN)$_2$]$_2$. Also, complex **2**, observed to be mononuclear, was observed to have a hydrogen-bonding network, with this feature being specific to pyrimidine-type complexes due to the additional noncoordinating N atoms.

Table 2 Bond lengths of complex **2**

Average bond lengths/Å		
T/K	296(2)	90(2)
Fe–N_{ligand}	2.264(6)	2.252(5)
Fe–N_{cyano}	2.130(6)	2.127(6)
Fe–O	2.104(5)	2.112(4)
Au–C	1.980(7)	1.977(7)
Au–Au	3.441	3.391

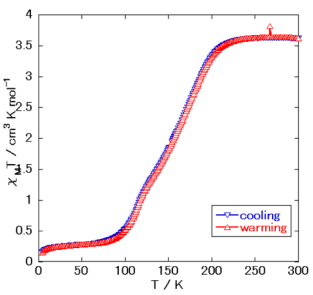

Fig. 4 Magnetic susceptibility of complex **1**.

Conclusions

We have synthesized a novel Soma–Iwamoto-type complex, Fe(quinazoline)$_2$[Au(CN)$_2$]$_2$ (**1**). Complex **1** shows a double-layered structure and a two-step SCO phenomenon. Also, analysis of a single crystal of Fe(H$_2$O)$_2$(quinazoline)$_2$[Au(CN)$_2$]$_2$ (complex **2**) obtained using the filter method shows a mononuclear complex and a hydrogen-bonding network. The difference between the structures could be explained by different quinazoline concentrations during their syntheses. Complex **1** and previously reported complex Fe(isoquinoline)$_2$[Au(CN)$_2$]$_2$ are isostructural, yet show different SCO behaviors.

Conflicts of interest

There are no conflicts to declare.

Notes and references

‡ Crystal data of complex **1**: $C_{20}H_{12}N_8FeAu_2$, M = 814.23 g mol^{-1}, CCDC reference number: 2332163 (296 K), 2332164 (150 K) and 2332165 (100 K).† That of complex **2**: $C_{20}H_{16}N_8O_2FeAu_2$, M = 850.26 g mol^{-1}, CCDC reference number: 2332161 (296 K) and 2332162 (90 K).†

1 K. A. Hofmann and F. Z. Küspert, Verbindungen von Kohlenwasserstoffen mit Metallsalzen, *Z. Anorg. Chem.*, 1897, **15**, 204.
2 T. Kitazawa, Y. Gomi, M. Takahashi, M. Takeda, M. Enomoto, A. Miyazaki and T. Enoki, Spin-crossover behaviour of the coordination polymer $Fe^{II}(C_5H_5N)_2Ni^{II}(CN)_2$, *J. Mater. Chem.*, 1996, **6**, 119.
3 T. Soma, H. Yuge and T. Iwamoto, Three-Dimensional Interpenetrating Double and Triple Framework Structures in [Cd(bpy)$_2${Ag(CN)$_2$}$_2$] and [Cd(pyrz){Ag$_2$(CN)$_3$}{Ag(CN)$_2$}], *Angew. Chem., Int. Ed. Engl.*, 1994, **33**, 1665–1666.
4 T. Soma and T. Iwamoto, Variations of multi-dimensional supramolecular structures built of the two-dimensional [Cd(py)$_2${Ag(CN)$_2$}$_2$]$_n$ network: Three-dimensional textile structures of catena-poly[trans-bis(pyridine)cadmium(II)-di-μ-{dicyanoargentato(I)-N,N′}]·G (G = benzene or pyrrole) and

two-dimensional layer structure of catena-poly[trans-bis(pyridine)cadmium(II)-di-μ-{dicyanoargentato(I)-N,N′}], *J. Inclusion Phenom. Macrocyclic Chem.*, 1996, **26**, 161–173.

5 S. Nishikiori, T. Soma and T. Iwamoto, In-plane and Out-of-plane Motion of Benzene Trapped in a $Cd(py)_2\{Ag(CN)_2\}_2$ Host as Studied by Deuterium NMR, *J. Inclusion Phenom. Macrocyclic Chem.*, 1997, **27**, 233–243.

6 V. Niel, J. M. Martínez-Agudo, M. C. Muñoz, A. B. Gaspar and J. A. Real, Cooperative Spin Crossover Behavior in Cyanide-Bridged Fe(II)–M(II) Bimetallic 3D Hofmann-like Networks (M = Ni, Pd, and Pt), *Inorg. Chem.*, 2001, **40**, 3838–3839.

7 K. Yoshida, D. Akahoshi, T. Kawasaki, T. Saito and T. Kitazawa, Guest-dependent spin crossover in a Hofmann-type coordination polymer Fe(4,4′-bipyridyl)$[Au(CN)_2]_2$·nGuest, *Polyhedron*, 2013, **66**, 252–256.

8 Y.-C. Chen, Y. Meng, Y.-J. Dong, X.-W. Song, G.-Z. Huang, C.-L. Zhang, Z.-P. Ni, J. Navařík, O. Malina, R. Zbořil and M.-L. Tong, Light- and temperature-assisted spin state annealing: accessing the hidden multistability, *Chem. Sci.*, 2020, **11**, 3281–3289.

9 Z. Feng, J.-J. Ling, H. Song and D. Zhu, Modulation of the spin transition in 2D Hofmann frameworks via π···π stacking between the axial 2,5-dipyridyl-1,3,4-oxadiazoles, *New J. Chem.*, 2023, **47**, 10162–10168.

10 A. Martinez-Martinez, E. Resines-Urien, N. S. Settineri, S. J. Teat, E. C. Sañudo, O. Fabelo, J. A. Rodriguez-Velamazan, L. Piñeiro-López and J. S. Costa, Two-Step Spin Crossover 3D Hofmann-Type Coordination Polymers Including a Functional Group in the Organic Moiety, *Cryst. Growth Des.*, 2023, **23**(6), 3952–3957.

11 R. Kosuge, T. Kawasaki, K. Kitase and T. Kosone, The Synthesis and Crystal Structures of New One- and Two-Dimensional Fe(II) Coordination Polymers Using Imidazole Derivatives, *Crystals*, 2023, **13**(12), 1658.

12 A. Galet, M. C. Muñoz, A. B. Gaspar and J. A. Real, Architectural Isomerism in the Three-Dimensional Polymeric Spin Crossover System $\{Fe(pmd)_2[Ag(CN)_2]_2\}$: Synthesis, Structure, Magnetic Properties, and Calorimetric Studies, *Inorg. Chem.*, 2005, **44**, 8749–8755.

13 K. Kitase and T. Kitazawa, A novel two-step Fe–Au type spin-crossover behavior in a Hofmann-type coordination complex $\{Fe(4\text{-methylpyrimidine})_2[Au(CN)_2]_2\}$, *Dalton Trans.*, 2020, **49**, 12210–12214.

14 K. Kitase, D. Akahoshi and T. Kitazawa, Effects of both methyl and pyrimidine groups in Fe–Ag spin-crossover Hofmann-type complex $\{Fe(4\text{-methylpyrimidine})_2[Ag(CN)_2]_2\}$, *Inorg. Chem.*, 2021, **60**, 4717–4722.

15 K. Kitase, D. Akahoshi and T. Kitazawa, Guest-triggered "Soma–Iwamoto-type" penetration complex $\{Fe(4\text{-methoxypyrimidine})_2[M(CN)_2]_2\}$·Guest (M = Ag, Au), *Dalton Trans.*, 2023, **52**, 2571–2579.

16 W. Dong, L.-N. Zhu, Y.-Q. Sun, M. Liang, Z.-Q. Liu, D.-Z. Liao, Z.-H. Jiang, S.-P. Yana and P. Cheng, 3D porous and 3D interpenetrating triple framework structures constructed by aurophilicity-coordination interplay in $\{Mn[Au(CN)_2]_2(H_2O)_2\}_n$ and $\{KFe[Au(CN)_2]_3\}_n$, *Chem. Commun.*, 2003, 2544–2545.

17 G. M. Sheldrick, *Acta Crystallogr., Sect. C: Struct. Chem.*, 2015, **71**, 3–8.

18 G. M. Sheldrick, *Acta Crystallogr., Sect. A: Found. Crystallogr.*, 2008, **64**, 112–122.